RSC Advances

RSC Publishing

PAPER

View Article Online
View Journal | View Issue

Cite this: *RSC Advances*, 2013, **3**, 16387

$KSrScSi_2O_7:Eu^{2+}$: a novel near-UV converting blue-emitting phosphor with high efficiency and excellent thermal stability†

Sudeshna Ray,[a] Ying-Chien Fang[b] and Teng-Ming Chen*[a]

Received 10th May 2013,
Accepted 1st July 2013

DOI: 10.1039/c3ra42882f

www.rsc.org/advances

A novel blue-emitting phosphor $KSrScSi_2O_7:Eu^{2+}$, synthesized from a water-soluble propylene glycol modified silane (PGMS) silicon precursor by a solution approach, exhibits high internal quantum efficiency and remarkable thermal stability, which are attributed to the rigid structural network of the host and weak electron–phonon coupling strength.

Introduction

White-light emitting diodes, the so called next-generation solid-state lighting, offer benefits in terms of high energy efficiency, durability, reliability and safety, and, most importantly, energy saving and therefore they can replace conventional incandescent and fluorescent lamps.[1] Owing to their reduced power use, LEDs in conjugation with renewable energy sources also offer great promise in providing lighting in remote and underdeveloped areas of the world.[2] Towards these ends, the Optoelectronics Industry Development Association (OIDA) plans to achieve 200 lm W^{-1} efficacy with good color rendering by 2020.[3] To achieve this goal, new phosphors with high efficiencies are the key. The most frequently used n-UV excitable blue phosphor is $BaMgAl_{10}O_{17}:Eu^{2+}$ (BAM), whose absorption in the n-UV region is poor;[4] as a consequence, investigations into the development of a new n-UV excitable blue-emitting phosphor has become essential. Host selection is an important factor in this development process. For the exploration of a new phosphor we adopt a ''mineral inspired methodology''. Among different possible matrices, silicates are good candidates to serve as the host structure due to several merits such as excellent chemical and thermal stability and their abundance in nature, they constitute approximately 90% of the crust of the earth. Interestingly, the number of known inorganic silicates is over 14 000, most of which have been derived from natural minerals, and this substantiates the significance of the mineral inspired approach. For example, rankinite ($Ca_3Si_2O_7$),[5] jervisite ($NaScSi_2O_6$),[6] wastromite ($BaCa_2Si_3O_9$),[7] akermanite ($Ca_2MgSi_2O_7$),[8] anorthite ($CaAl_2Si_2O_8$),[9] or pyrope ($Mg_3Al_2(SiO_4)_3$)],[10] doped with a rare-earth ion, can act as an efficient phosphor. The large number of phosphors derived from minerals evidences the fact that this ''mineral inspired methodology'' for developing a new phosphor is advantageous and less time-consuming than the combinational method developed by a generic algorithm.[11] Apart from this approach, another fact that needs to be documented is that, until now, the reported silicate phosphors were mainly synthesized by a conventional high-temperature solid-state reaction methodology,[12–14] which has some drawbacks such as the volatility and low-melting point of the starting materials and possible side reactions eventually fail to produce the desired compounds. On the contrary, the solution process has a number of advantages like achieving the homogenous mixing of the starting materials on the atomic level as well as obtaining complex silicates with precisely-controlled compositions. Furthermore, the uniform distribution of the activator in the host matrix, can avoid potential concentration quenching and the consequent depression of the emission intensity.[15] But, the solution synthesis of silicates is difficult due to the insolubility of silicates. Among various solution methods,[16,17] the low-temperature synthesis of functional silica glass by the so-called sol–gel method using tetraethoxysilane (TEOS) as a raw material[18] has been reported. However, using TEOS as a source of Si makes the synthesis of complex silicates with a precisely controlled chemical composition quite difficult due to the possible evaporation of TEOS during the solvent elimination process. In this study, we use a water-soluble silicon compound, known as ''propylene glycol modified silane'' (PGMS), to serve as a source of Si[19–21] facilitating a convenient synthesis technique for complex silicates by employing an appropriate solution-based approach. Furthermore, PGMS does not suffer from the evaporation problem like TEOS, which makes this reagent more beneficial

[a]*Department of Applied Chemistry, National Chiao Tung University, Hsinchu 30010, Taiwan (ROC). E-mail: tmchen@mail.nctu.edu.tw; Fax: 886+35723764; Tel: 886+35731695*

[b]*Department of Chemical Engineering, National Taiwan University, Taipei 10617, Taiwan (ROC). E-mail: ycf1981@gmail.com*

† Electronic supplementary information (ESI) available. See DOI: 10.1039/c3ra42882f

during the synthesis of complex silicates with precisely controlled stoichiometry.

In 2010, a high-temperature flux growth-mediated synthesis of a novel scandium silicate $KSrScSi_2O_7$ (KSS) was detailed.[22] In the present study, for the first time, we explain that the $KSrScSi_2O_7$ compound synthesized by an amorphous metal complex (AMC) method, a solution based approach using a water-soluble silicon compound, can be used as a blue emitting phosphor when doped with 2% Eu^{2+}, which shows an internal quantum efficiency (IQE) higher than 80% and excellent thermal stability. In this report, the solution synthesis, phase identification of the compound by X-ray diffraction (XRD), photoluminescence (PL) measurements and thermal quenching of the luminescence, and in particular, the comparison of the performance of KSS:Eu^{2+} (2%) with the commercially available BAM phosphor are presented. We also suggest explanations for the unusual thermal stability of the KSS:Eu^{2+} phosphor.

Experimental section

In a typical synthesis, $SrCO_3$, $Sc(NO_3)_3$ and $Eu(NO_3)_3$ solutions along with citric acid, which actually acts as a complexing agent, were used. PGMS, which was used as a source of Si, was obtained by an alkoxy group exchange reaction with tetra-hydroxy silane (TEOS) in the presence of an acid as a catalyst.[15] Fig. 1 presents the reaction between TEOS and propylene glycol (PG), in the presence of an acid catalyst to generate PGMS.

For the synthesis of PGMS, 0.4 mol of PG (Kanto Chemical 99.9%) and 0.1 mol of TEOS (Kanto Chemical, 99.9%) were transferred by a digital pipette into a 100 mL conical flask with a stopper. As TEOS is insoluble in PG, the liquid mixture was divided into two phases. 100 μL of concentrated hydrochloric acid (HCl, Kanto Chemical, 36%) was added as a catalyst for the alkoxy group exchange reaction. The mixture was magnetically stirred at 80 °C for 1 h which resulted in the formation of a transparent uniform solution without any phase separation. This solution can be mixed with water in any ratio without hydrolysis of the silicon compound. This compound is called PGMS. It was transferred into a 100 mL volumetric flask and diluted with distilled water to obtain a 1 M PGMS solution. The AMC method includes different steps

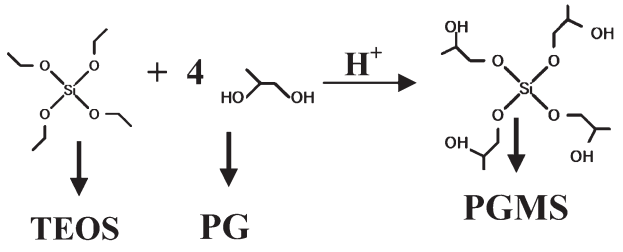

Fig. 1 Reaction between TEOS and PG in the presence of an acid catalyst to produce PGMS.

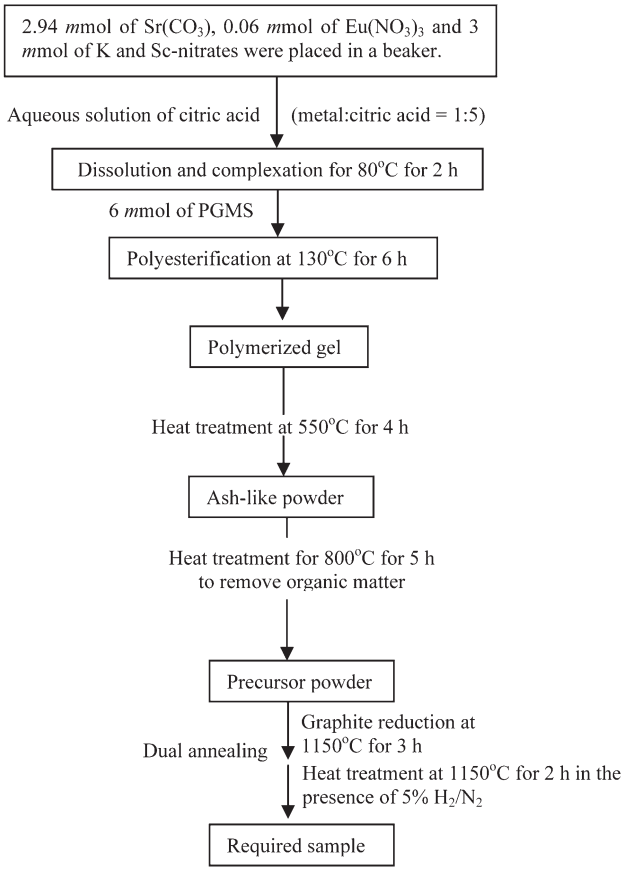

Fig. 2 Flow chart describing the AMC method for the synthesis of $KSr_{0.98}Eu_{0.02}ScSi_2O_7$.

like polyesterification at 130 °C for 6 h, several heat treatment steps at 450 °C for 12 h, 550 °C for 4 h and 800 °C for 5 h to obtain the precursor. Finally the precursor was heat treated at 1150 °C for 3 h under graphite reduction conditions followed by heat treatment at 1150 °C for 2 h under H_2/N_2 atm. The synthesis procedure has been detailed in the flow chart diagram shown in Fig. 2.

Material characterization

The crystal structure of the as-synthesized sample was identified by using powder X-ray diffraction (XRD) analysis with a Bruker AXS D8 advanced automatic diffractometer with Cu-Kα radiation (λ = 1.5418 Å), over the angular range $10^\circ \leqslant 2\theta \leqslant 80^\circ$, operating at 40 kV and 40 mA. The photoluminescence (PL) and PL excitation (PLE) spectra of the samples were analyzed by using a Spex Fluorolog-3 Spectrofluorometer equipped with a 450-W Xe light source. The temperature dependent PL spectra were obtained with a spectrophotometer (Jobin-Yvon Spex, Model FluoroMax-3).

Results and discussion

Since the uniform distribution of activator ions into the host matrix is the key factor responsible for the enhancement of the

luminescence intensity of the phosphor, the above-mentioned "AMC" method has several advantages, as follows: 1) the complexation of the cations by citric acid greatly improved the stability of the initial solution against hydrolysis or precipitation, which increases the local activator concentration and eventually diminishes the emission intensity of the phosphor. 2) The dissolution of Sc_2O_3 in nitric acid has been difficult and to the best of our knowledge, for the first time we report the synthesis of $[Sc(NO_3)]_3$ by the prolonged heat treatment (about 7 days) of Sc_2O_3 in concentrated HNO_3 in the presence of distilled water at 80 °C under constant stirring. 3) The water evaporation facilitates the formation of a gel with a high viscosity, in which, the mobility of the metal ions is lowered,[18] which, in turn is responsible for the prohibition of the undesirable segregation of metal ions. It is important to mention that an aqueous solution of PGMS undergoes self-gelation and solidifies if the hydrolysis of PGMS proceeds very slowly.[20] To get an improved uniformity of the dopant ion in the matrix, self-gelation of PGMS is detrimental as it would increase the local activator concentration. In the AMC method, after the addition of PGMS, two competitive gelation processes take place simultaneously, the reaction of PGMS with the metal-citrate precursor along with self-gelation of PGMS. It has been reported that the hydrolysis of PGMS proceeds quickly with increased temperature, which in turn decreases the self-gelation of PGMS.[20] For this reason, the temperature of the hot plate was raised to 130 °C to suppress the self-gelation process at the expense of the reaction of PGMS with the metal-citrate precursor. It should be mentioned that in this synthesis, the precursor has been annealed in a graphite atmosphere at 1150 °C for 3 h followed by being reduced in a H_2/N_2 atmosphere at the same temperature. This "double annealing" has a crucial effect on the emission intensity of the final product. Instead of "double annealing", heat treatment of the precursor in a H_2/N_2 atmosphere for 5 h, resulted in the formation of the product along with some impurity phases, whereas in the double annealing strategy, the crystal structure was stabilized after the graphite reduction. Once the crystal has been formed, the heat treatment in a H_2/N_2 atmosphere does not produce any impurity phases, although this process significantly increases the emission intensity of the phosphor.

Fig. S1 ESI† presents the crystal structure of monoclinic $KSrScSi_2O_7$ with space group symmetry $P2_1/m$. The framework structures of tetrahedra and octahedra are based on an isolated Si_2O_7 group connected to octahedrally coordinated Sc cations, nine-coordinated Sr cations and eight-coordinated K cations. Adjacent ScO_6 octahedra are connected to each other through a Si_2O_7 unit, and interestingly, this connection forms the layers of ScO_6 polyhedra and furthermore a three-dimensional framework with Sr and K cations located in the voids.[22] Moreover, the Sr and K atoms are arranged with an alternating –Sr–K–Sr–K sequence. The most striking feature of the structure of KSS is that the diffusion of the cations in this direction is not possible as the cation-containing voids are separated by bottlenecks in the framework.[22] This demonstrates the rigidity of the crystal structure of KSS. Fig. 3

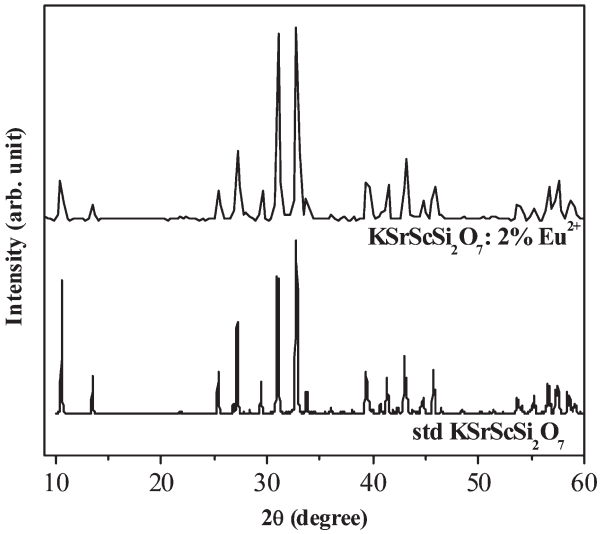

Fig. 3 Powder XRD patterns of $KSrScSi_2O_7:Eu^{2+}$.

displays the X-ray diffraction profile of the sample ($KSr_{0.98}Eu_{0.02}ScSi_2O_7$) which can be indexed to a pure monoclinic phase of $KSrScSi_2O_7$. Traces of impurity phases have not been found in the XRD patterns of the doped sample.

Fig. 4 presents the PL spectra of KSS:Eu^{2+} under the excitation of 365 nm. The spectra show a blue-emitting band peaking at 437 nm with color coordinates (0.15, 0.05). The PL intensity of KSS:Eu^{2+} was found to be 83.6% and 75.23% with respect to commercially available BAM under 365 nm and 400 nm excitations, respectively.

The optical absorbance (φ) and quantum efficiency (η) are calculated by using the following equations.[23]

$$\varphi = \frac{L_o(\lambda) - L_i(\lambda)}{L_o(\lambda)} \quad (1)$$

$$\eta = \frac{E_i(\lambda) - (1-\varphi)E_o(\lambda)}{E_o(\lambda)\varphi} \quad (2)$$

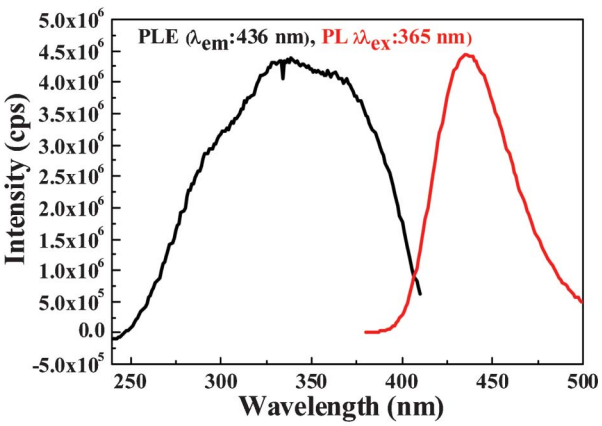

Fig. 4 PLE and PL spectra of $KSrScSi_2O_7:Eu^{2+}$.

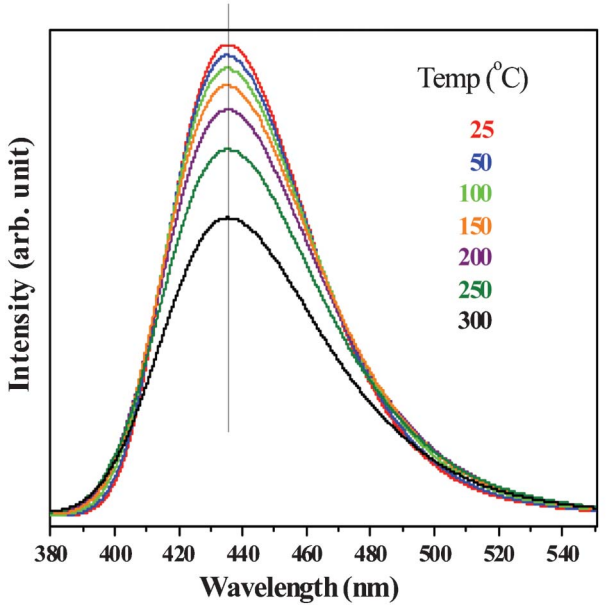

Fig. 5 Temperature-dependent PL spectra of $KSrScSi_2O_7:Eu^{2+}$.

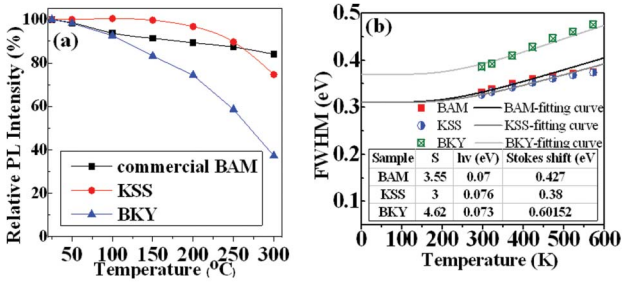

Fig. 6 (a) Temperature dependence of the relative integral PL intensity of Eu^{2+} doped KSS, BAM and BKY samples. (b) Temperature dependence of FWHM of Eu^{2+} doped KSS, BAM and BKY samples.

where $L_o(\lambda)$ is the integrated excitation profile when sample is diffusely illuminated by the integrated excitation profile when sample is directly excited by the incident beam, $E_o(\lambda)$ is the integrated luminescence of sample upon direct excitation, $E_i(\lambda)$ is the integrated luminescence of sample excited by indirect illumination from the sphere and $L_I(\lambda)$ is the integrated excitation profile obtained from the empty integrated sphere (without the sample present). Upon excitation at 365 nm, the optical absorbance (φ) of KSS:Eu^{2+} and BAM:Eu^{2+} have been calculated to be 42.41% and 74.3%, respectively. The internal quantum efficiency (η) of KSS:Eu^{2+} and BAM:Eu^{2+} were found to be 84.3% and 87.9% and the corresponding external quantum efficiency of these two samples are 35.75% and 65.31% respectively.

Temperature-dependent PL spectra of KSS:Eu^{2+} measured at 25–300 °C under excitation at 356 nm are presented in Fig. 5. The surface temperature of the current-driven LED chips on which the phosphors are mounted is around 120 °C. Interestingly, the PL intensity of KSS:Eu^{2+} at 150 °C retains 99.6% of that measured at room temperature (Fig. 4), which is much higher than that for BAM:Eu^{2+} (91.3%) as presented in Fig. 6(a).

The thermal quenching temperature (T_{50}) is defined as the temperature at which the PL intensity is 50% of its original value. At 300 °C, as shown in Fig. 6(a), KSS:Eu^{2+} retains 73.6% of its room temperature emission intensity, which indicates that T_{50} of this compound is above 300 °C. The most significant observation is the enhancement of the PL emission intensity of KSS:Eu^{2+} from 50 °C to 100 °C. This is attributed to the ''thermally activated'' transition of photo-excited electrons into the higher 5d level, at which the possibility of nonradiative transition may decrease, resulting in the rise of PL intensity. Although from Fig. 5, this enhancement is not very clear, this enhancement of the PL intensity is substantiated by the measurement of the area of the PL spectra taken at different temperatures. Similar phenomena have been observed for $LaSi_3N_5:Ce^{3+}$ and $CaEuAl_{2-x}Si_xO_{4-x}$.[24,25] With increasing temperature, the population density of phonons increased, and the electron–phonon interaction is dominant, which results in broadening of the emission spectra.[26] However, to investigate if the structural rigidity of KSS is responsible for its thermal stability or not, an isotypic compound of KSS,[27] $BaKYSi_2O_7$:2% Eu^{2+} (BKY) has been synthesized by the AMC method and the corresponding XRD is presented in Fig. S2 ESI.† It has been observed that at 150 °C, BKY retains 83.2% of its room temperature emission intensity (Fig. 6(a)), which indicates that the thermal stability of this compound is also sufficiently high. To investigate the difference in thermal quenching behaviour between these samples, the full width at half maximum (FWHM) of the emission spectra under various measurement temperatures, denoted as FWHM (T), were analyzed using MATLAB software. The FWHM (T) of Eu^{2+}-activated BAM, KSS and BKY samples are shown in Fig. 6(b). The FWHM (T) of the emission spectra can be described using the configurational coordinate model and the Boltzmann distribution according to the following equation.[28]

$$\text{FWHM}\ (T) = h\nu[8 \times \ln 2 \times S \times \coth(h\nu/2k_BT)]^{1/2} \quad (3)$$

where $h\nu$ is the mean phonon energy, S is the Huang–Rhys factor, and k_B is Boltzmann constant. The Huang–Rhys parameter S is the electron–phonon coupling strength. The Stokes shift (ΔS) can be estimated from $(2S - 1) \times h\nu = \Delta S$. According to eqn (3), the best fit to the emission sites of BAM is obtained with S = 3.55, $h\nu$ = 0.07 eV, and ΔS = 0.427 eV, as shown in Fig. 6(b).

For KSS, the best fit was obtained with S = 3, $h\nu$ = 0.076 eV, and ΔS = 0.38 eV. For BKY, the best fit was obtained with S = 4.62, $h\nu$ = 0.073 eV, and ΔS = 0.60152 eV. It has been reported that the small thermal quenching of BKY is ascribed to the rigid network of the compound.[27] From a structural viewpoint, although the KSS and BKY samples have the same structure, the bond angles and the bond lengths of KSS are smaller than those of BKY.[22,27] It indicates that KSS has a more rigid

structure leading to a lower thermal vibration or less thermal-loss energy at higher temperature. In the present work, we stress the point that KSS exhibits a weaker electron–phonon coupling, lower Stokes shift, and its structure is more rigid than that of BKY. From Fig. 6(a) and 6(b), it is evident that the thermal stability of KSS:Eu^{2+} is also superior to that of commercial BAM.

Conclusion

In conclusion, we have synthesized a single-phased $KSrScSi_2O_7$:2% Eu^{2+} by a facile solution-based approach using a water-soluble silicon compound as a precursor. The $KSrScSi_2O_7$:Eu^{2+} exhibits blue broadband emission peaking at 437 nm with high internal quantum efficiency (83.4%). Comparison of the thermal stability of KSS with that of the isostructural BKY phosphor indicates that the superior thermal stability of KSS is owed to its more rigid structural network. The thermal stability of KSS:Eu^{2+} is also attributed to a small Stokes shift, weak electron–phonon coupling strength, and lower phonon energy of this compound.

Acknowledgements

S. R. and T. M. C. acknowledge financial support from the National Science Council of Taiwan, R. O. C. under contract No. NSC101-2811-M-009-055 and NSC101-2113-M-009-021-MY3, respectively.

Notes and references

1 T. Hasimoto, F. Wu, J. S. Speck and S. Nakamura, *Nat. Mater.*, 2007, **6**, 568.
2 W. B. Im, S. Brinkley, J. Hu, A. Mikhailovsky, S. P. DenBaars and R. Seshadri, *Chem. Mater.*, 2010, **22**, 2842.
3 S. C. Allen and A. J. Steckl, *Appl. Phys. Lett.*, 2008, **92**, 1433091.
4 B. Howe and A. L. Diaz, *J. Lumin.*, 2004, **109**, 51.
5 F. Qian, R. Fu, S. Agathopoulos, X. Gu and X. Song, *J. Lumin.*, 2012, **132**, 71.
6 S. Merlino and P. Orlandi, *Period Mineral.*, 2006, **75**, 189.
7 S. Yao, L. Xue and Y. Yan, *Opt. Laser Technol.*, 2011, **43**, 1282.
8 L. Jiang, C. Chang, D. Mao and C. Feng, *Opt. Mater.*, 2004, **27**, 51.
9 J. K. Park, J. M. Kim, E. S. Oh and C. H. Kim, *Electrochem. Solid-State Lett.*, 2005, **8**, H6.
10 T. Ohagaki, A. Higashida, K. Soga and A. Yasumori, *J. Electrochem. Soc.*, 2007, **154**, J163.
11 A. K. Sharma, C. Kulshreshtha and K. S. Sohn, *Adv. Funct. Mater.*, 2009, **19**, 1705.
12 W. J. Yang, L. Luo, T. M. Chen and N. S. Wang, *Chem. Mater.*, 2005, **17**, 3883.
13 W. B. Im, Y. I. Kim and D. Y. Jeon, *Chem. Mater.*, 2006, **18**, 1190.
14 J. K. Park, K. J. Choi, J. H. Yeon, S. J. Lee and C. H. Ki, *Appl. Phys. Lett.*, 2006, **88**, 0435111.
15 M. Kakihana, *J. Ceram. Soc. Jpn.*, 2009, **117**, 857.
16 P. A. Trusty and C. B. Ponton, *Acta Mater.*, 1999, **47**, 779.
17 Y. Liu, C.-N. Xu, H. Matsui, T. Imamura and T. Watanabe, *J. Lumin.*, 2000, **87–89**, 1297.
18 P. J. Marsh, J. Silver, A. Vecht and A. Newport, *J. Lumin.*, 2002, **97**, 229.
19 Y. Suzuki and M. Kakihana, *J. Ceram. Soc. Jpn.*, 2009, **117**, 857.
20 K. Yoshizawa, H. Kato and M. Kakihana, *J. Mater. Chem.*, 2012, **22**, 17272.
21 C. Yasushita, H. Kato and M. Kakina, *J. Inf. Disp.*, 2012, **13**, 107.
22 M. Wierzbicka-Wieczorek, U. Kolitsch and E. Tillmanns, *Can. Mineral.*, 2010, **48**, 51.
23 J. C. de Mello, H. F. Wittmann and R. H. Friend, *Adv. Mater.*, 1997, **9**, 230.
24 T. Suehiro, N. Hirosaki, R.-J. Xie and T. Sato, *Appl. Phys. Lett.*, 2009, **95**, 051903.
25 Y. C. Fang, P. C. Kao and S. Y. Chu, *J. Electrochem. Soc.*, 2011, **158**, J120.
26 J. S. Kim, Y. H. Park, S. M. Kim, J. C. Choi and H. L. Park, *Solid State Commun.*, 2005, **133**, 445.
27 U. Kolitsch, M. Wierzbicka-Wieczorek and E. Tillamans, *Can. Mineral.*, 2009, **47**, 421.
28 D. W. Cooke, B. L. Bennett, K. J. Maclellan, J. M. Roper and M. T. Whittaker, *J. Appl. Phys.*, 2000, **87**, 7793.